EurJIC
European Journal of Inorganic Chemistry

A Journal of ChemPubSoc Europe

Accepted Article

Title: New Mixed-C^N Ligand Tris-cyclometalated Ir(III) Complexes for Highly-Efficient Green Organic Light-Emitting Diodes with Low Efficiency Roll-off

Authors: Xiaoyu Ma, Jie Liang, Fuquan Bai, Kaiqi Ye, Jianing Xu, Dongxia Zhu, and Martin Robert Bryce

To be cited as: *Eur. J. Inorg. Chem.* 10.1002/ejic.201800550

Link to VoR: http://dx.doi.org/10.1002/ejic.201800550

WILEY-VCH

New Mixed-*C^N* Ligand Tris-cyclometalated Ir(III) Complexes for Highly-Efficient Green Organic Light-Emitting Diodes with Low Efficiency Roll-off

Xiaoyu Ma[a], Jie Liang[b], Fuquan Bai[a], Kaiqi Ye[a,*], Jianing Xu[a], Dongxia Zhu[c,*], Martin R. Bryce [d,*]

[a] *College of Chemistry, Jilin University, 2699 Qianjin Street, Changchun 130012, P. R. China.*

[b] *State Key Laboratory of Supramolecular Structure and Materials, Institute of Theoretical Chemistry, Jilin University, 2699 Qianjin Street, Changchun 130012, P. R. China.*

[c] *Institute of Functional Material Chemistry, Faculty of Chemistry, Northeast Normal University, 5268 Renmin Road, Changchun, 130024, P. R. China.*

[d] *Department of Chemistry, Durham University, Durham DH1 3LE, UK*

Abstract

This article reports new tris-cyclometalated Ir(III) complexes containing mixed-*C^N* ligands, $(C^{\wedge}N_1)_2Ir(C^{\wedge}N_2)$, which are a rarely explored class of complexes. Two mixed 2-phenylpyridine (ppy) / 4-methyl-2,5-diphenylpyridine (mdp) complexes $(ppy)_2Ir(mdp)$ **3** and $(ppy)Ir(mdp)_2$ **4** have been synthesized and their optoelectronic properties have been systematically characterized. Photoluminescence quantum yield values are 0.76–0.85; excited state lifetimes are 0.07–0.11 μs. Phosphorescent organic light emitting devices (PhOLEDs) based on these emissive complexes in a very simple device architecture reproducibly showed slightly higher external quantum efficiency (EQE) and power efficiency (PE) values compared with devices using the analogous conventional homoleptic Ir complexes $Ir(ppy)_3$ and $Ir(mdp)_3$, and the heteroleptic complexes $(ppy)_2Ir(acac)$ and $(mdp)_2Ir(acac)$. The new complexes $(ppy)_2Ir(mdp)$ **3** and $(ppy)Ir(mdp)_2$ **4** give PhOLEDs with EQE_{max} and PE_{max} values of 26.7 and 26.0% / 94.7 and 94.1 lm W^{-1}, respectively, and very high

values are retained at the practical luminances of 100 and 1000 cd m^{-2}. The values for $(ppy)_2Ir(mdp)$ are 26.3% and 73.6 lm W^{-1} (at 100 cd m^{-2}) and 24.6% and 53.5 lm W^{-1} (at 1000 cd m^{-2}). These efficiencies are comparable with the highest reported values of PhOLEDs using conventional Ir(III) emitters in more complicated device structures. Mixed *C^N* ligand systems are, therefore, a viable strategy for developing new efficient phosphorescent emitters.

Keywords

Iridium complex, Mixed-*C^N* ligand, Cyclometalation, OLED, Electrophosphorescence

Introduction

Cyclometalated iridium(III) complexes possess rich metal-ligand based photophysical properties, notably short phosphorescent lifetimes, high quantum efficiencies and good stability, which has led to their extensive use in a range of optoelectronic applications, notably as emissive dopants in phosphorescent organic light-emitting diodes (PhOLEDs).[1-7] During the last 20 years a vast number of experimental and theoretical studies have focused on the design, synthesis and characterization of different classes of Ir complexes leading to improved materials and device structures, as well as to enhanced efficiencies and brightness of PhOLEDs.[8-12] Correspondingly, there are hundreds of homoleptic tris-cyclometalated Ir complexes $Ir(C^N)_3$ (*C^N* = cyclometalated ligand) based on the parent $Ir(ppy)_3$ structure (ppy = 2-phenylpyridine).[13,14] Heteroleptic Ir complexes $(C^N)_2Ir(LX)$ incorporating ancillary ligands (*LXs*) such as acetylacetonate (acac), picolinate, triazolate and amidinate derivatives have also been widely developed, especially in the context of tuning the emission color.[15-17] However, there is only very limited information on tris-cyclometalated Ir complexes containing *mixed C^N* ligands, $(C^N_1)_2Ir(C^N_2)$ as these species have only rarely been characterized.[18,19] We are aware of only one complex of this type being used as an emitter in PhOLEDs: very low efficiency orange electroluminescence was reported for a non-optimized PhOLED of $Ir(ppy)_2(fppy)$ [fppy = 2-(4'-formylphenyl)pyridine].[18] Thus, this class of phosphors has great scope for development as a fundamental structural motif for organoiridium(III) complexes.

In this work, we prepared the new complexes **3**-**6** with systematic changes of the ligands [ppy

and 4-methyl-2,5-diphenylpyridine (mdp)] and their relative ratio. These complexes [$(ppy)_2Ir(mdp)$ (**3**), $(ppy)Ir(mdp)_2$ (**4**), $Ir(mdp)_3$ (**5**) and $(mdp)_2Ir(acac)$ (**6**) are compared with the well-known complexes $(ppy)_2Ir(acac)$ (**1**) and $Ir(ppy)_3$ (**2**). Complexes **3-6** have been synthesized in good yields, and characterized by cyclic voltammetry, optical absorption and photoluminescence studies, density functional theory (DFT) calculations, and by single-crystal X-ray diffraction studies (for **3**, **4** and **6**). PhOLEDs fabricated using complexes **1-6** as the emitters, doped in a 4,4'-bis(*N*-carbazolyl)biphenyl (CBP) host, give efficient EL emission in the green region, achieving very high EL performance with maximum power efficiencies (PEs) of >80 lm W^{-1} and >20% external quantum efficiencies (EQEs). A notable feature is that the highest values have been achieved in the PhOLEDs employing complexes **3** and **4** which possess mixed-$C^{\wedge}N$ ligand structures, with EQE_{max} and PE_{max} values of 26.7 and 26.0% / 94.7 and 94.1 lm W^{-1}, respectively, and with low roll-off of EQE to 1000 cd m^{-2}. These values are consistently and reproducibly higher than those of the other four devices: i.e. those with $(C^{\wedge}N)_2Ir(LX)$ complexes **1** and **6**, or the $Ir(C^{\wedge}N)_3$ complexes **2** and **5** as the emitter.

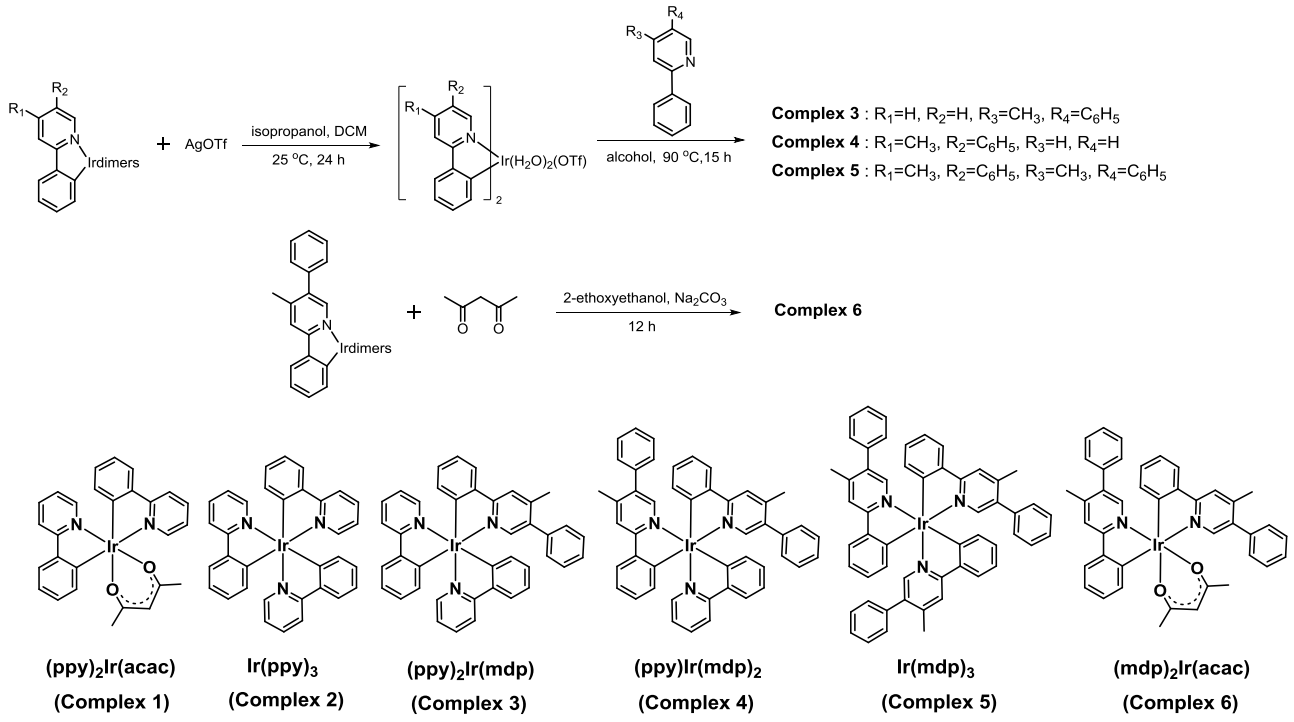

Scheme 1. The synthetic routes to complexes **3-6** and the chemical structures of complexes **1-6**.

Results and Discussion

Synthesis of complexes

Scheme 1 depicts the synthetic routes to complexes **3-6**, based on established protocols.[20,21,22] The complexes were characterized by ^{1}H NMR spectroscopy, mass spectrometry and elemental analysis which unambiguously confirmed their structures. The facial isomers of the mixed-C^N ligand complexes **3** and **4** had been obtained in ~60% yield as the kinetically favoured products.[23-25] X-ray crystallography shows the facial structures (see below).

Thermal Properties

The thermal properties of complexes **3-6** were examined by thermogravimetric analysis (TGA) and differential scanning calorimetry (DSC). These complexes possess high decomposition temperatures (T_d, corresponding to 5% weight loss) of >380 °C (**Figure 1**) and melting points (T_m) >370 °C. Such excellent thermal properties are desirable for emitting phosphors as they can suppress aggregation and phase separation, and thereby ensure the high morphological stabilities and amorphous characteristics in the solid film state which are very important for the thermal stability of the complexes during device operation and for high efficiency and lifetime of OLEDs.[2,4]

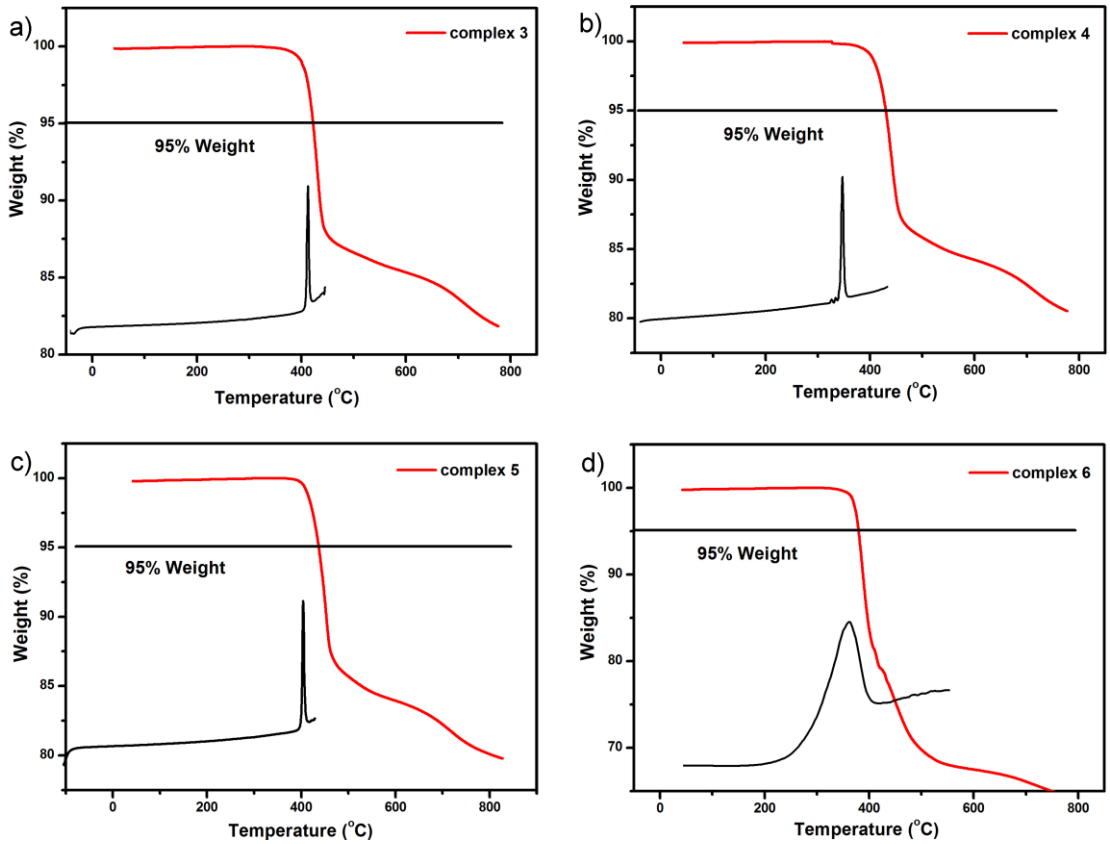

Figure 1. Thermal analyses of complexes **3**-**6**: thermogravimetric analysis (TGA, red line) and differential scanning calorimetry (DSC, black line).

Table 1. Photophysical, and electrochemical data for complexes **3**-**6.**

Complex	λ_{max}^{abs} / nm[a]	λ_{max}^{em} / nm[a,b]	PLQY / Φ_{PL}[c]	τ_P / μs[a,d]	k_r / 10^6 s^{-1}	k_{nr} / 10^6 s^{-1}	HOMO / LUMO / eV[e]	T_1 / eV[f]
3	286, 378, 458	519[a], 514[b]	0.77	0.11	7.01	2.09	-4.91/-2.47	2.41
4	289, 383, 463	523[a], 517[b]	0.77	0.08	9.61	2.87	-4.91/-2.46	2.39
5	291, 389, 458	524[a], 518[b]	0.76	0.07	1.10	3.43	-4.89/-2.45	2.39
6	278, 348, 467	521[a], 520[b]	0.85	0.11	0.77	1.36	-5.01/-2.59	2.38

[a] Data obtained in dichloromethane solution at 20 °C. [b] Data obtained in toluene solution at 77 K. [c] Measured in degassed DCM at 20 °C (error ±5%). [d] Estimated error ±5%. [e] Measured in DCM (0.1 M Bu_4NPF_6) at 298 K. [f] Estimated from the onset wavelengths of the 77 K emission spectra measured in toluene solution.

Photophysical and Electrochemical Properties

Steady-state ultraviolet–visible (UV–vis) absorption spectra of complexes **3**-**6** in dilute dichloromethane solution (2.0×10^{-5} M) are shown in **Figure 2a** and the data are summarized in **Table 1**. The intense absorption bands peaking around 278–291 nm are attributed to the spin-allowed intraligand centered (LC) transitions,[22] while the relatively weaker and broad absorption bands from 330–550 nm with lower extinction coefficients are primarily ascribed to ^{1}MLCT (metal-to-ligand charge-transfer), ^{1}LLCT (ligand-to-ligand charge-transfer), ^{3}MLCT, ^{3}LLCT, and ligand-centered (LC) $^3\pi$-π^* transitions.[26] The photoluminescence (PL) spectra were obtained at room temperature using an excitation wavelength of 365 nm. As shown in **Figure 2b**, the PL maxima and profiles are all very similar indicating that tuning the *C^N* ligands and/or introducing the *LX* ligand has only a minimal effect on the emission color of the complexes. The broad and largely featureless emission profiles indicate that efficient spin–orbit coupling leads to intersystem crossing from the singlet to triplet states resulting in a strong MLCT contribution to the emission.[27] All the four complexes exhibit green emission, with λ_{max} values in the range of 519–524 nm and with quantum yield values of 0.76–0.85, which are higher than the well-known complex $Ir(ppy)_3$ (**2**) (~0.40).[27] This is because of their shorter lifetimes (0.07–0.11 μs) compared to $Ir(ppy)_3$, which are beneficial for increasing spin-state mixing and decreasing the triplet exciton aggregation, thus leading to the relatively high PLQYs and also reducing the efficiency roll-off in

the EL process.[28] The triplet levels were obtained from the emission spectra at 77 K recorded in toluene solution (Figure S9).

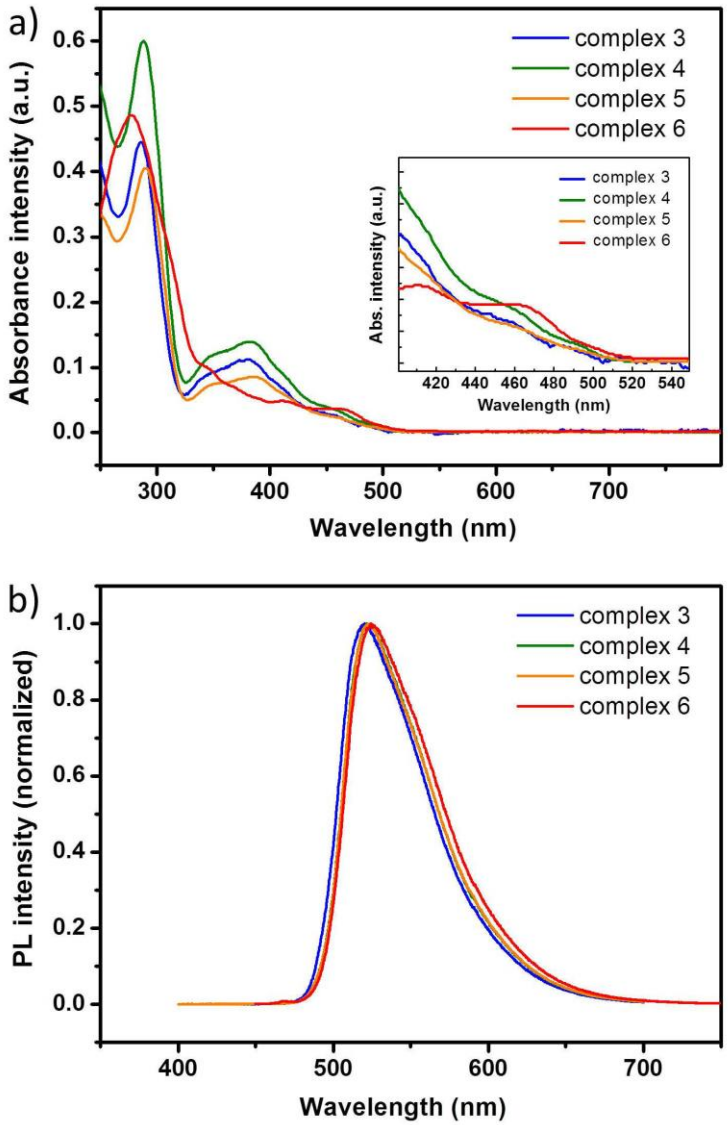

Figure 2. a) Absorption and b) PL spectra of complexes **3-6** in DCM solution at room temperature. The insert in a) is an expansion of the 400−550 nm region.

The cyclic voltammetry (CV) data were measured to investigate the electrochemical features and estimate the highest occupied molecular orbital (HOMO) and lowest unoccupied molecular orbital (LUMO) energy levels of the complexes **3-6**. The electrochemical data are summarized in **Table 1**. As shown in **Figure 3**, all the complexes show an electrochemically quasi/irreversible oxidation at 0.32–0.43 V vs Fc/Fc^+, assigned to the Ir(III)/Ir(IV) couple; the onset oxidation potentials of complexes **3-5** are similar. The HOMO levels were calculated from the onset of the

oxidation potential according to the equation $E_{HOMO/LUMO} = -(E_{[onset,ox/red\ vs\ Fc+/Fc]} + 4.8)$ eV.[29] No reduction features were observed within the solvent window (scanning to -1.5 V vs Fc/Fc^+), thus the LUMO levels of the four complexes were determined by considering the difference between their HOMO levels and the corresponding HOMO–LUMO gaps (E_g) which were calculated from the absorption edge of their UV-vis spectra. The HOMO and LUMO values are found to be –4.91 and –2.47 eV for **3**, –4.91 and –2.46 eV for **4**, –4.89 and –2.45 eV for **5**, –5.01 and –2.59 eV for **6**, which result in very similar HOMO–LUMO gaps (E_g) in agreement with the computational results below. The raised HOMO level and less reversible process for complex **6** are due to the ancillary acac ligand.

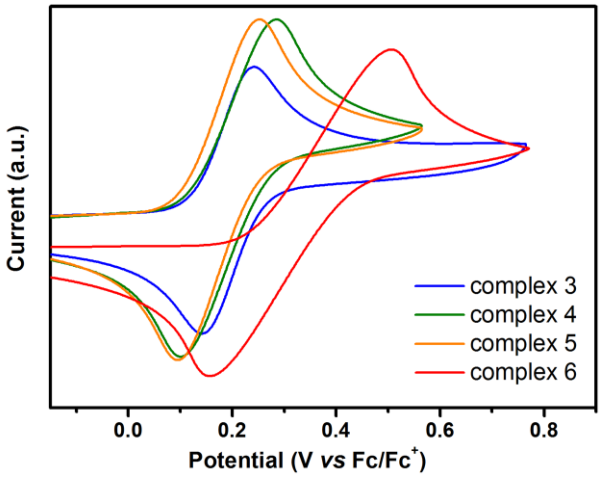

Figure 3. Cyclic voltammograms of complexes **3-6** in deaerated DCM.

X-ray Crystallography and Theoretical Calculations

To further understand the structural features of these complexes, single crystals of complexes **3**, **4** and **6** were characterized by X-ray crystallography. The crystal structures are shown in **Figure 4** and the crystal data are listed in **Table S1**. Complexes **3**, **4** and **6** all have distorted octahedral geometry around the iridium center which is surrounded by three C^N ligands, as previously reported for tris-cyclometalated Ir complexes (**Figure 4a**).[30,31] The facial isomers are observed for **3** and **4**, which typically endows higher quantum efficiencies compared to meridional isomers.[32] In the structure of complex **3**, the molecules are connected into molecular chains along the *c* axis by C-H···π interactions with contact distances of 2.695 Å. The molecules in the crystal of complex **4** are also held together through weak C-H···π interactions (2.855 Å). In the case of complex **6**, the

molecules are assembled into molecular chains with intermolecular hydrogen bonding interactions (2.699 Å) between oxygen atoms of the acac groups and hydrogen atoms on adjacent phenyl rings.

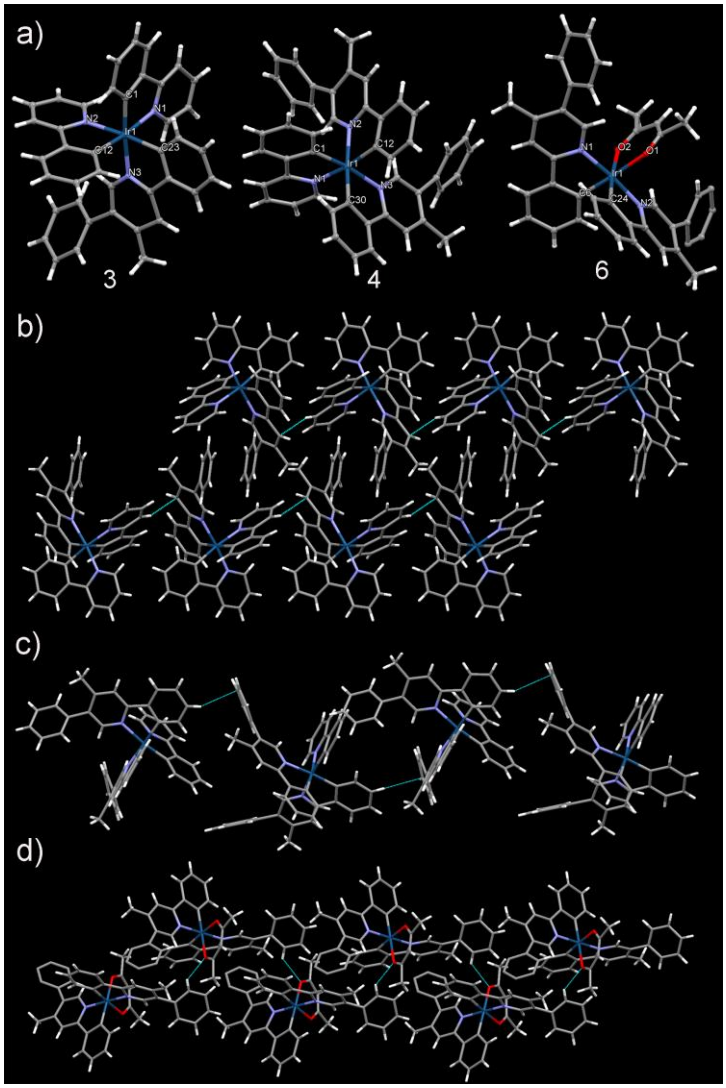

Figure 4. a) X-ray molecular structures of complexes **3**, **4** and **6**. b) and c) Molecular chains driven by C-H···π interactions in the crystals of complexes **3** and **4**. d) C-H···O hydrogen bonds in complex **6**. These interactions are shown as green lines.

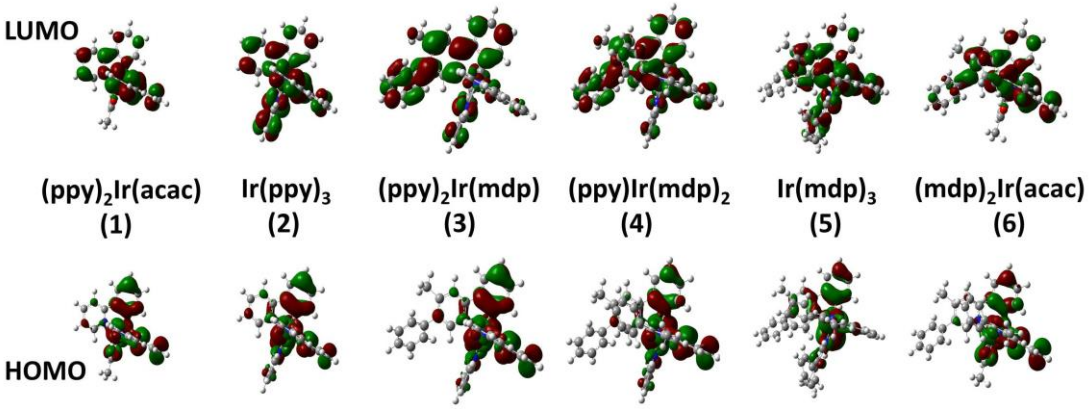

Figure 5. Molecular orbital diagrams of compounds **1-6**.

Table 2. HOMO and LUMO levels and MOs on the complexes from DFT calculations.

		Energy	MO composition (%)			
	Orbital	(eV)	Ir	L1	L2	L3
1	HOMO	-5.49	52	15 (ppy)	24 (ppy)	9 (acac)
	LUMO	-3.36	5	12 (ppy)	82 (ppy)	2 (acac)
2	HOMO	-5.40	56	14 (ppy)	15 (ppy)	15 (ppy)
	LUMO	-2.31	2	33 (ppy)	29 (ppy)	36 (ppy)
3	HOMO	-6.68	53	18 (ppy)	19 (ppy)	10 (mdp)
	LUMO	-3.55	2	80 (ppy)	6 (ppy)	12 (mdp)
4	HOMO	-6.98	53	18 (mdp)	20 (mdp)	9 (ppy)
	LUMO	-3.89	1	54 (mdp)	35 (mdp)	9 (ppy)
5	HOMO	-6.28	42	42 (mdp)	7 (mdp)	9 (mdp)
	LUMO	-3.17	2	18 (mdp)	75 (mdp)	5 (mdp)
6	HOMO	-5.46	52	13 (mdp)	26 (mdp)	9 (acac)
	LUMO	-2.01	2	29 (mdp)	68 (mdp)	1 (acac)

Density functional theory (DFT) was used to rationalize the fundamental properties of these iridium complexes, and to provide a theoretical foundation to supplement experiments to design related phosphorescent Ir(III) complexes. The full geometrical configurations were optimized at the B3LYP/LANL2DZ:6-31G* level. **Figure 5** depicts the electron density distributions of the HOMOs and LUMOs of complexes **1-6**. They display similar HOMO and LUMO frontier orbital distributions, except for complex **2**. The HOMO orbitals of complexes **1**, **3**, **4**, **5** and **6** are distributed over the π* orbitals of the C^N cyclometalated ligands (ppy or mdp) (39, 37, 38, 49 and 39%, respectively), with a large contribution from the π orbitals of the iridium atom (52, 53, 53, 42 and 52%, respectively). The LUMO orbitals of complexes **1**, **3**, **4**, **5** and **6** are mostly localized on π orbitals of both cyclometalated ligands (>90%) together with a fraction of the d-orbitals of the iridium atom and ancillary ligands (<10%) **(Table 2)**. In contrast, the HOMO frontier orbital of complex **2** is localized largely on the π orbitals of the iridium atom (56%) and almost equally on the three ppy ligands, while the LUMO is located throughout the three ppy ligands. These data are consistent with previous theoretical calculations on complexes **1** and **2**.[33]

Electrophosphorescent devices

To explore the EL performance of PhOLEDs employing new complexes **3-6** as dopant emitters, four devices, namely **D3**, **D4**, **D5** and **D6** respectively, were fabricated in the following uniform and simple configuration: ITO/NPB (40 nm)/doped EML (8 wt% complex in CBP, 30 nm)/TPBi (30 nm)/LiF (0.5 nm)/Al], where the corresponding phosphors were coevaporated with a well-matched energy gap host molecule 4,4-bis(*N*-carbazolyl)-1,1'-biphenyl (CBP) as the emitting layer (EML). 4,4'-Bis(*N*-(1-naphthyl)-*N*-phenylamino)biphenyl (NPB) served as a hole-transporting layer (HTL) and 1,3,5-tris(*N*-phenylbenzimidazol-2-yl)benzene (TPBi) as an electron-transporting layer (ETL) (**Figure 6a**). For comparison, the devices **D1** and **D2** with the same device configuration were fabricated by using complexes **1** and **2** as the dopant, respectively. All the six PhOLEDs **D1-D6** present bright green emission with λ_{max} at 520-528 nm at the brightness of 1000 cd m^{-2} (**Figure 6b and Table 3**). These λ_{max} values are consistent with the photoluminescence (PL) spectra (**Figure 2b**). The EL spectrum of each device is very stable under a range of driving voltages (5-9 V) (Figure S10), and no additional emission from the host was observed. This confirms that complete and effective energy transfer occurs from CBP host to phosphor dopant.

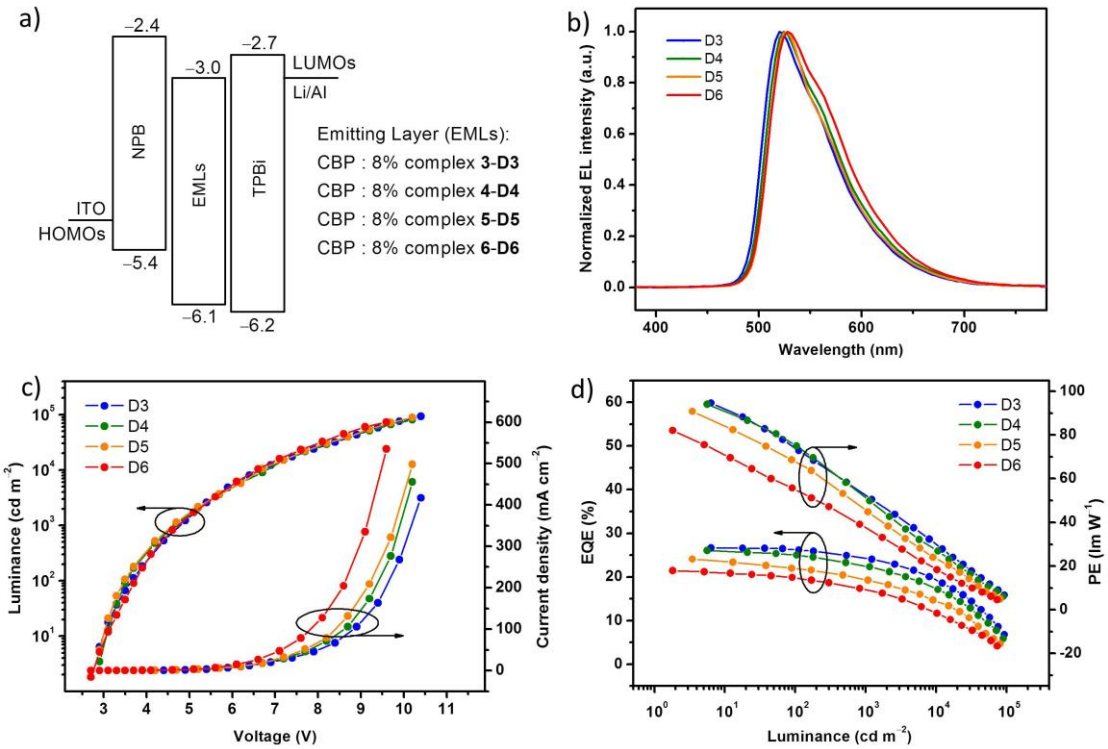

Figure 6. a) Energy diagram of the materials used in the PhOLEDs. b) EL spectra of **D3**, **D4**, **D5** and **D6** at the practical luminance of 1000 cd m^{-2}. c) Current density-voltage-luminance (*J*-*V*-*L*)

curves of **D3**, **D4**, **D5** and **D6**. d) Power efficiency (PE)-luminance (L)-external quantum efficiency (EQE) curves of **D3**, **D4**, **D5** and **D6**.

Figures 6c and **6d** show the current density-voltage-luminance (*J–V–L*), external quantum efficiency (*EQE–L*) and power efficiency-luminance (*PE–L*) characteristics of the devices **D3-D6**. For comparison, the key device data of devices **D1-D6** are summarized in **Table 3**. All the devices exhibit rapidly increasing *J*−*V* and *L*−*V* curves based on low turn-on voltages (recorded at ≥1 cd m^{-2}) of 2.7−2.9 V, and the driving voltages needed to reach the practical luminances of 100 and 1000 cd m^{-2} are 3.5-3.8 V and 4.6-4.9 V, respectively. Moreover, at relatively low driving voltages of 6.6-6.9 V, an extremely high luminance of >10,000 cd m^{-2} was obtained for all the devices **D3-D6**. The low operating voltage with the rapid increase of current and luminance indicates that effective hole injection occurs from the HOMO of the HTL (NPB) and electron injection from the LUMO of the ETL (TPBi), respectively. All six devices **D1-D6** achieved the high peak EQE and PE values of >20% / 75 lm W^{-1} with low roll-off. Among them, **D3** and **D4** based on complexes **3** and **4** containing the mixed-*C*^*N* ligands of ppy and mdp, consistently showed higher EQE/PE than the other four devices, in terms of their peak values of 26.7 and 26.0% / 94.7 and 94.1 lm W^{-1}, and reduced roll-off (**Figure 6d**). For **D3** and **D4** the very high levels of 26.3 and 25.1% / 73.6 and 74.7 lm W^{-1}, 24.6 and 22.7% / 53.5 and 51.6 lm W^{-1} were attained at the practical luminances of 100 and 1000 cd m^{-2}, respectively. The consistent 10-15% increase in EL efficiencies (EQE and PE) of **D3** and **D4**, compared to the tris-homoleptic analogs **D2** and **D5**, is based on the average performance of three parallel device fabrications / measurements. On each occasion **D3** and **D4** out-performed **D2** and **D5** which clearly points to a significant benefit of the mixed-*C*^*N* ligand structures. These high efficiencies of **D3** and **D4** with a simple HTL/EML/ETL device structure and commercially available host and transport layer materials, are comparable with the highest reported levels of PhOLEDs employing the classical homoleptic or heteroleptic Ir complexes $Ir(ppy)_3$ (**2**) or $(ppy)_2Ir(acac)$ (**1**), respectively, using more complicated and refined device structures, and/or non-commercial host or co-host materials.[34-38] More significantly, the direct comparison of devices **D1**-**D6** in the present work convincingly demonstrates that high-level EL performance of the classical homoleptic and heteroleptic phosphors can be maintained, and even slightly enhanced, with tris-cyclometalated Ir complexes with mixed-*C*^*N* ligands. Hence, mixed-ligand Ir complexes

are worthy of further study and should no longer be overlooked in testing new phosphors for efficient PhOLEDs.

We are aware of only one previous example of a PhOLED of a tris-cyclometalated Ir complex containing mixed *C^N* ligands: very low efficiency orange EL was observed in a non-optimized single-layer device.[18] There is now the prospect that the EL performance of complexes containing mixed *C^N* ligands may be further optimized through molecular structure modifications, or technologies such as integrating micro/nano patterns, stretchable substrate, single-crystal EML and dual-periodicity metallic electrodes.[39-42]

Speculative reasons for the enhanced PhOLED performance of complexes **3** and **4** compared to **2** and **5** are a favorable alignment of the transition dipoles of **3** and **4**, due to their mixed *C^N* ligand structure, and this could lead to enhanced outcoupling efficiencies compared to **2** and **5** which comprise three identical *C^N* ligands.[43,44] Also there may be favorable host-guest supramolecular interactions in the emitting layers of **D3** and **D4**, again facilitated by the asymmetry of the complexes **3** and **4**.[45]

Table 3. EL data of the devices **D1-D6**.

Device	$V_{turn\text{-}on}$ [a] / V	L_{max} / cd m^{-2} (V at L_{max})	PE [b] / lm W^{-1}	EQE [b] / %	$EL\ \lambda_{max}$ [c] / nm	$CIE_{x,y}$ [c]
D1	2.7	69420 (9.7)	77.5, 56.8, 41.5	20.7, 19.7, 17.9	520	(0.33, 0.60)
D2	2.9	87750 (10.9)	87.6, 63.1, 44.2	24.7, 23.0, 21.1	520	(0.33, 0.60)
D3	2.9	92800 (10.4)	94.7, 73.6, 53.5	26.7, 26.3, 24.6	520	(0.33, 0.60)
D4	2.9	89480 (10.2)	94.1, 74.7, 51.6	26.0, 25.1, 22.7	524	(0.34, 0.60)
D5	2.9	80950 (10.2)	82.5, 66.3, 46.6	23.4, 21.8, 19.5	524	(0.34, 0.60)
D6	2.7	73530 (9.6)	82.2, 55.1, 38.3	21.4, 19.7, 17.1	528	(0.35, 0.60)

[a] Recorded at ≥1 cd m^{-2}. [b] In the order of maximum, then values at 100 and 1000 cd m^{-2}. [c] Measured at 1000 cd m^{-2}.

Conclusions

In summary, a series of four new Ir phosphors comprising two mixed 2-phenylpyridine (ppy) / 4-methyl-2,5-diphenylpyridine (mdp) tris-cyclometalated complexes $(ppy)_2Ir(mdp)$ (**3**) and $(ppy)Ir(mdp)_2$ (**4**), one homoleptic complex $Ir(mdp)_3$ (**5**), and one $(C^N)_2Ir(LX)$ complex $(mdp)_2Ir(acac)$ (**6**) have been rationally developed and systematically characterized. PhOLEDs based on complexes **3** and **4** containing mixed *C^N* ligands are shown to have consistently higher

EQE/PE values (by 10-15%) than the other four devices using the conventional homoleptic complexes $Ir(ppy)_3$ and $Ir(mdp)_3$, or heteroleptic complexes $(ppy)_2Ir(acac)$ and $(mdp)_2Ir(acac)$. The EL efficiencies and brightness of **D3** and **D4** in a simple device architecture are comparable with the highest efficiencies of previously reported PhOLEDs for standard homoleptic and heteroleptic Ir(III) complexes employing more complicated and elaborate device structures. There is very limited information in the literature about tris-cyclometalated Ir complexes containing mixed $C^{\wedge}N$ ligands. There is clearly scope for using the efficient synthetic methodology employed in this work to extensively vary the $C^{\wedge}N$ ligands which will give new opportunities to study the impact of two different cyclometalated ligands on the fundamental photophysics of Ir complexes.[46,47] Also, as a consequence of the excellent EL performance demonstrated here, new $(C^{\wedge}N_1)_2Ir(C^{\wedge}N_2)$-type emitters may be exploited in displays and solid-state lighting applications.

Experimental Section

Materials and Instrumentation: All starting materials and solvents were commercially available and used as received without further purification. Complexes **1** and **2** were purchased from Xi'an Polymer Light Technology Corporation. All manipulations were performed under a dry nitrogen atmosphere using standard techniques. ^1H NMR spectra were measured on an AVANCE 600 MHz spectrometer (Bruker) with $CDCl_3$ and tetramethylsilane (TMS) as the internal standard. Mass spectra were recorded on a GC/MS mass spectrometer (Thermo Fisher). Elemental analyses were obtained on a Vario Micro elemental analyzer. Thermal gravimetric analysis (TGA) and differential scanning calorimetry (DSC) characteristics were determined under nitrogen atmosphere with a TA Q500 thermogravimeter and a NETZSCH DSC204 instrument using a heating rate of 10 °C min^{-1}. Ultraviolet−visible (UV−vis) absorption spectra were obtained with a Shimadzu UV-2550 spectrophotometer. The PL emission spectra were recorded by using an Edinburgh fluorescence spectrometer (FLS 920) with an integrating sphere. Solution PLQYs were recorded in degassed solvent by using quinine sulfate (Φ_{PL} = 0.546 in 0.5 M H_2SO_4) as the reference. Cyclic voltammetry measurements were performed in anhydrous CH_2Cl_2 using a BAS 100W bioanalytical electrochemical workstation with a platinum (Pt) electrode as working electrode, a porous glass wick Ag/Ag^+ electrode as the reference electrode, and a Pt wire as the counter electrode. The oxidation potentials were measured at a scan rate of 100 mV s^{-1} in a 0.1 M solution of dry dichloromethane using Bu_4NPF_6 as a supporting electrolyte.

The synthesis of 4-methyl-2,5-diphenylpyridine (mdp) and $[(mdp)_2Ir(\mu\text{-}Cl)]_2$ is given in the Supporting Information.

Synthesis of complex 3: $[(ppy)_2Ir(\mu\text{-}Cl)]_2$ (5.36 g, 5.0 mmol) and $Ag(CF_3SO_3)$ (2.83 g, 11.0 mmol) were added into CH_2Cl_2 (100 mL) and isopropanol (27 mL). The mixture was stirred at 25 °C for 24 h then washed with dichloromethane, affording a yellow solid (7.06 g) in 99% yield which was separated by filtration. A mixture of this intermediate product (3.57 g, 5.0 mmol) and 4-methyl-2,5-diphenylpyridine (mdp) (3.67 g, 15.0 mmol) in ethanol (80 mL) was heated at reflux for 15 h under nitrogen. The reaction solution was cooled to room temperature and the resulting mixture was washed with dichloromethane, affording complex **3** as a yellow solid (2.16 g, 58% yield). ESI-MS: m/z 744.84 (M^+) (calcd: 745.21). Anal. Calcd for $C_{40}H_{30}IrN_3$: C, 64.50; H, 4.06; N, 5.64. Found: C, 64.38; H, 3.83; N, 5.63. ^{1}H NMR (600 MHz, $CDCl_3$) δ 7.90 (d, *J* = 12.0 Hz, 1H), 7.85 (d, *J* = 6.0 Hz, 1H), 7.76 (s, 1H), 7.69–7.72 (m, 3H), 7.60–7.64 (m, 2H), 7.52 (t, *J* = 18.0 Hz, 1H), 7.47 (d, *J* = 6.0 Hz, 1H), 7.30–7.37 (m, 4H), 7.10 (d, *J* = 6.0 Hz, 2H), 6.82–6.94 (m, 7H), 6.77 (t, *J* = 12.0 Hz, 2H), 6.67–6.74 (m, 2H), 2.40 (s, 3H). Single crystals for X-ray analysis were grown by vacuum vapor deposition.

Synthesis of complex 4: The synthesis of complex **4** was similar to that of complex **3**, where a mixture of the intermediate product based on $[(mdp)_2Ir(\mu\text{-}Cl)]_2$ (7.16 g, 5.0 mmol) and $Ag(CF_3SO_3)$ (2.83 g, 11.0 mmol) were added into CH_2Cl_2 (100 mL) and isopropanol (27 mL). The mixture was stirred at 25 °C for 24 h then washed with dichloromethane, affording a yellow solid (8.81 g) in 99% yield which was separated by filtration. A mixture of this intermediate product (4.47 g, 5.0 mmol) and and ppy (2.33 g, 15.0 mmol) in ethanol (80 mL) was heated at reflux for 15 h under nitrogen. After the reaction solution was cooled to room temperature, the resulting mixture was washed with dichloromethane, affording complex **4** as a yellow solid (2.59 g, 62% yield). ESI-MS: m/z 834.90 (M^+) (calcd: 835.25). Anal. Calcd for $C_{47}H_{36}IrN_3$: C, 67.60; H, 4.35; N, 5.03. Found: C, 67.40; H, 4.24; N, 5.04. ^{1}H NMR (600 MHz, $CDCl_3$) δ 7.85 (d, *J* = 6.0 Hz, 1H), 7.77 (s, 1H), 7.66–7.71 (m, 4H), 7.58 (d, *J* = 6.0 Hz, 1H), 7.52 (t, *J* = 18 Hz, 1H), 7.48 (s, 1H), 7.30–7.38 (m, 7H), 7.15 (d, *J* = 6.0 Hz, 2H), 7.00 (d, *J* = 6.0 Hz, 2H), 6.87–6.91 (m, 6H), 6.81–6.86 (m, 4H), 2.41 (s, 3H), 2.29 (s, 3H). Single crystals for X-ray analysis were grown by vacuum vapor deposition.

Synthesis of complex 5: The synthesis of complex **5** was similar to that of complex **4.** A mixture of

the yellow solid intermediate product (4.47 g, 5.0 mmol) and mdp (3.68 g, 15.0 mmol) in ethanol (80 mL) was heated at reflux for 15 h under nitrogen. After the reaction solution was cooled to room temperature, the resulting mixture was washed with dichloromethane, affording complex **5** as a yellow solid (2.68 g, 58% yield). ESI-MS: m/z 925.3 (M^+) (calcd: 924.87). Anal. Calcd for $C_{54}H_{42}IrN_3$: C, 70.11; H, 4.58; N, 4.54. Found: C, 70.02; H, 4.45; N, 4.54. ^{1}H NMR (600 MHz, $CDCl_3$) δ 7.70 (s, 3H), 7.65 (d, *J* = 6.0 Hz, 3H), 7.44 (s, 3H), 7.30–7.35 (m, 9H), 7.00–7.02 (m, 6H), 6.89–6.95 (m, 9H), 2.30 (s, 9H).

Synthesis of complex 6: A mixture of $[(mdp)_2Ir(\mu\text{-}Cl)]_2$ (2.86 g, 2.0 mmol), Na_2CO_3 (1.06 g, 10.0 mmol), acetylacetone (1.0 g, 10.0 mmol) and 2-ethoxyethanol (100 mL) were heated at reflux for 12 h under nitrogen. The reaction solution was cooled to room temperature and the resulting mixture was washed with dichloromethane, affording complex **6** as a yellow solid (0.78 g, 50% yield). ESI-MS: m/z 779.88 (M^+) (calcd: 780.23). Anal. Calcd for $C_{41}H_{35}IrN_2O_2$: C, 63.02; H, 4.39; N, 3.61. Found: C, 63.14; H, 4.52; N, 3.59. ^{1}H NMR (600 MHz, $CDCl_3$) δ 8.40 (s, 2H), 7.73 (s, 2H), 7.56 (d, *J* = 6 Hz, 2H), 7.46–7.49 (m, 4H), 7.39–7.42 (m, 6H), 6.82 (t, *J* = 12 Hz, 2H), 6.72 (t, *J* = 12 Hz, 2H), 6.38 (d, *J* = 6.0 Hz, 2H), 5.22 (s, 1H), 2.58 (s, 6H), 1.72 (s, 6H). Single crystals for X-ray analysis were grown by vacuum vapor deposition.

Acknowledgments

Dr. X. Y. Ma and J. Liang contributed equally to the work reported in this article. This work was supported by National Key Research and Development Plan of China (2017YFB0404400) and Natural Science Foundation of China (51773078 and 51473028). The work in Durham was supported by EPSRC grant EP/K039423/1.

Supporting Information for this article is available on the WWW under https://doi.org/xxxxx

References

[1] M. A. Baldo, D. F. O'Brien, Y. You, A. Shoustikov, S. Sibley, M. E. Thompson, S. R. Forrest, *Nature* **1998**, *395*, 151-154.

[2] (a) Y. You, W. Nam, *Chem Soc Rev.* **2012**, *41*, 7061-7084. (b) S. Guo, T. Huang, S. Liu, K. Zhang, H. Yang, J. Han, Q. Zhao, W. Huang, *Chem. Sci.* **2017**, *8*, 348-360.

[3] R. Mertens, *The OLED Handbook. A Guide to OLED Technology, Industry and Market* **2014**: www.oled-info.com/handbook.

[4] (a) S. Ladouceur, E. Zysman-Colman, *Eur. J. Inorg. Chem.* **2013**, *17*, 2985-3007. (b) J. Han, S. Guo, J. Wang, L. Wei, Y. Zhuang, S. Liu, Q. Zhao, X. Zhang, W. Huang, *Adv. Opt. Mater.* **2017**, *5*, 1700359.

[5] (a) H. Sasabe, J. Kido, *J. Mater. Chem. C* **2013**, *1*, 1699-1707. (b) P. Tao, Y. Zhang, J. Wang, L. Wei, H. Li, X. Li, Q. Zhao, X. Zhang, S. Liu, H. Wang, W. Huang, *J. Mater. Chem. C* **2017**, *5*, 9306-9314.

[6] E. Zysman-Colman, *Dalton Trans.* **2015**, *44*, 8317-8317.

[7] (a) X. Yang, G. Zhou, W.Y. Wong, *Chem. Soc. Rev.* **2015**, *44*, 8484-8575. (b) P. Tao, W. Li, J. Zhang, S. Guo, Q. Zhao, H. Wang, B. Wei, S. Liu , X. Zhou, Q. Yu , B. Xu, W. Huang, *Adv. Funct. Mater.* **2016**, *26*, 881-894.

[8] H. Li, R. Bi, T. Chen, K. Yuan, R. Chen, Y. Tao, H. Zhang, C. Zheng, W. Huang, *ACS Appl. Mater. Interfaces* **2016**, *8*, 7274-7282.

[9] X. Zhuang, H. Zhang, K. Ye, Y. Liu, Y. Wang, *ACS Appl. Mater. Interfaces* **2016**, *8*, 11221-11225.

[10] Q. Zhang, D. Tsang, H. Kuwabara, Y. Hatae, B. Li, T. Takahashi, S. Y. Lee, T. Yasuda, C. Adachi, *Adv. Mater.* **2015**, *27*, 2096-2100.

[11] M. A. Baldo, M. E. Thompson, S. R. Forrest, *Nature* **2000**, *403*, 750-753.

[12] W. J. Finkenzeller, H. Yersin, *Chem. Phys. Lett.* **2003**, *377*, 299-305.

[13] Y. You, S. Y. Park, *J. Am. Chem. Soc.* **2005**, *127*, 12438-12439.

[14] E. Orselli, G. S. Kottas, A. E. Konradsson, P. Coppo, R. Fröhlich, L. De Cola, A. van Dijken, M. Büchel, H. Borrner, *Inorg. Chem.* **2007**, *46*, 11082-11093.

[15] Y. Liu, K. Ye, Y. Fan, W. Song, Y. Wang, Z. Hou, *Chem. Commun.* **2009**, 3699-3701.

[16] G. Li, D. Zhu, T. Peng, Y. Liu, Y. Wang, M. R. Bryce, *Adv. Funct. Mater.* **2014**, *24*, 7420-7426.

[17] Y. Feng, X. Zhuang, D. Zhu, Y. Liu, Y. Wang, M. R. Bryce, *J. Mater. Chem. C* **2016**, *4*,

10246-10252.

[18] A. Beeby, S. Bettington, I. D. W. Samuel, Z. Wang, *J. Mater. Chem.* **2003**, *13*, 80-83.

[19] K. Dedeian, J. Shi, N. Shepherd, E. Forsythe, D. C. Morton, *Inorg. Chem.* **2005**, *44*, 4445-4447.

[20] M. Nonoyama, *Bull. Chem. Soc. Jpn.* **1974**, *47*, 767-768.

[21] K. Dedeian, P. I. Djurovich, F. D. Garces, G. Carlson, R. J. Watts, *Inorg. Chem.* **1991**, *30*, 1685-1687.

[22] J. Li, P. I. Djurovich, B. D. Alleyne, I. Tsyba, N. N. Ho, R. Bau, M. E. Thompson, *Polyhedron* **2004**, *23*, 419-428.

[23] G. Park, Y. Kim, Y. Ha, *Mol. Cryst. Liq. Cryst.* **2006**, *462,* 179-188.

[24] (a) Y. Tamura, Y. Hisamatsu, S. Kumar, T. Itoh, K. Sato, R. Kuroda, S. Aoki, *Inorg. Chem.* **2017**, *56*, 812-833. (b) Y. Tamura, Y. Hisamatsu, A. Kazama, K. Yoza, K. Sato, R. Kuroda, S. Aoki, *Inorg. Chem.* **2018**, *57*, 4571-4589.

[25] M. Lepeltier, F. Dumur, B. Graffe, P. Xiao, D. Gigmes, J. Lalevée, C. R. Mayer, *Helv. Chim. Acta* **2014**, *97*, 939-956.

[26] S. Lamansky, P. Djurovich, D. Murphy, F. Abdel-Razzaq, R. Kwong, I. Tsyba, M. Bortz, B. Mui, R. Bau, M. E. Thompson, *Inorg. Chem.* **2001**, *40*, 1704-1711.

[27] A. Tsuboyama, H. Iwawaki, M. Furugori, T. Mukaide, J. Kamatani, S. Igawa, T. Moriyama, S. Miura, T. Takiguchi, S. Okada, M. Hoshino, K. Ueno, J. *Am. Chem. Soc.* **2003**, *125*, 12971-12979.

[28] T. Hofbeck, H. Yersin, *Inorg. Chem.* **2010**, *49*, 9290-9299.

[29] S.Wang, Z. Cheng, X. Song, X. Yan, K. Ye, Y. Liu, G. Yang, Y. Wang, *ACS Appl. Mater. Interfaces* **2017**, *9*, 9892-9901.

[30] M. O. BaniKhaled, J. D. Becker, M. Koppang, H. Sun, *Cryst. Growth Des.* **2016**, *16*, 1869-1878.

[31] Y. Zhao, X. Mu, C. Bao, Y. Fan, J. Zhang, Y. Wang, *Langmuir* **2009**, *25*, 3264-3270.

[32] A. B. Tamayo, B. D. Alleyne, P. I. Djurovich, S. Lamansky, I. Tsyba, N. N. Ho, R. Bau, M. E. Thompson, *J. Am. Chem. Soc.* **2003**, *125*, 7377-7387.

[33] P. J. Hay, *J. Phys. Chem. A* **2002**, *106*, 1634-1641.

[34] D. Tanaka, H. Sasabe, Y-J. Li, S.-J. Su, T. Takeda, J. Kido, *Jpn. J. Appl. Phys.* **2007**, *46*, L10-L12.

[35] S-J. Su, H. Sasabe, Y-J. Pu, K-i. Nakayama, J. Kido, *Adv. Mater.* **2010**, *22*, 3311-3316.

[36] T. Yang, H. Xu, Z. Xi, K. Wang, P. Tao, P. Sun, B. Zhao, Y. Miao, H. Lian, H. Wang, B. Xu, W.-Y. Wong, *Dyes and Pigments* **2017**, *146*, 582-588.

[37] X. Cai, R. Liu, H. Shi, C. Li, H. Zhu, *Dyes and Pigments* **2017**, *143*, 196-202.

[38] K. Gao, K. Liu, X.-L. Li, X. Cai, D. Chen, Z. Xu, Z. He, B. Li, Z. Qiao, D. Chen, Y. Cao, S.-J. Su, *J. Mater. Chem. C* **2017**, *5*, 10406-10416.

[39] J. Feng, Y. F. Liu, Y. G. Bi, H. B. Sun, *Laser Photon. Rev.* **2017**, *11*, 1600145.

[40] D. Yin, J. Feng, R. Ma, Y. F. Liu, Y. L. Zhang, X. L. Zhang, Y. G. Bi, Q. D. Chen, H. B. Sun, *Nat. Commun.* **2016**, *7*, 11573.

[41] R. Ding, J. Feng, X. L. Zhang, W. Zhou, H. H. Fang, Y. F. Liu, Q. D. Chen, H. Y. Wang, H. B. Sun, *Adv. Funct. Mater*. **2014**, *24*, 7085-7092.

[42] Y. G. Bi, J. Feng, Y. F. Li, X. L. Zhang, Y. F. Liu, Y. Jin, H. B. Sun, *Adv. Mater.* **2013**, *25*, 6969-6974.

[43] T. Lee, B. Caron, M. Stroet, D. M. Huang, P. L. Burn, A. E. Mark, *Nano Lett*. **2017**, *17*, 6464-6468.

[44] C.-K. Moon, K.-H. Kim, J. W. Lee, J.-J. Kim, *Chem. Mater.* **2015**, *27*, 2767-2769.

[45] T. Lampe, T. D. Schmidt, M. J. Jurow, P. I. Djurovich, M. E. Thompson, W. Brutting, *Chem. Mater.* **2016**, *28*, 712-715.

[46] R. M. Edkins, A. Wriglesworth, K. Fucke, S. L. Bettington, A. Beeby, *Dalton Trans.* **2011**, *40*, 9672-9678.

[47] E. Baranoff, B. F. E. Curchod, J. Frey, R. Scopelliti, F. Kessler, I. Tavernelli, U. Rothlisberger, M. Gratzel, M. K. Nazeeruddin, *Inorg. Chem.* **2012**, *51*, 215-224.

10.1002/ejic.201800550

Entry for Table of Contents

Rare examples of luminescent tris-cyclometalated iridium complexes with mixed *C^N* ligands have been characterized and shown to be efficient emitters in phosphorescent organic light-emitting diodes.

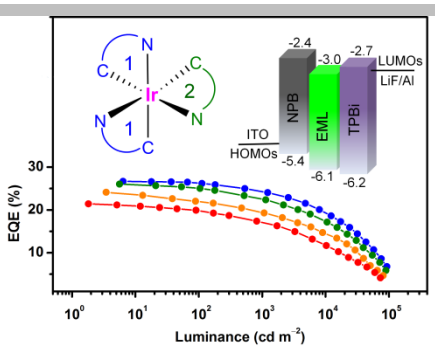

Luminescent complexes

*Author(s), Corresponding Author(s)**

Page No. – Page No.

Title

Supporting Information

New Mixed-*C*^*N* Ligand Tris-cyclometalated Ir(III) Complexes for Highly-Efficient Green Organic Light-Emitting Diodes with Low Efficiency Roll-off

Xiaoyu Ma[a], Jie Liang[b], Fuquan Bai[a], Kaiqi Ye[a,*], Jianing Xu[a], Dongxia Zhu[c,*], Martin R. Bryce [d,*]

[a] *College of Chemistry, Jilin University, 2699 Qianjin Street, Changchun 130012, P. R. China.*

[b] *State Key Laboratory of Supramolecular Structure and Materials, Institute of Theoretical Chemistry, Jilin University, 2699 Qianjin Street, Changchun 130012, P. R. China.*

[c] *Institute of Functional Material Chemistry, Faculty of Chemistry, Northeast Normal University, 5268 Renmin Road, Changchun, 130024, P. R. China.*

[d] *Department of Chemistry, Durham University, Durham DH1 3LE, UK*

Synthesis of ligand 4-methyl-2,5-diphenylpyridine (mdp)[1] (Scheme S1)

A mixture of 2,5-dibromo-4-methylpyridine (7.76 g, 30.92 mmol), phenylboronic acid (9.43 g, 77.31 mmol), K_2CO_3 (1.2 g, 9.0 mmol), $Pd(PPh_3)_4$ (0.71 g, 0.62 mmol) and toluene (180 mL) was heated to 90 °C for 12 h under a N_2 atmosphere. After cooling to room temperature, deionized water (200 mL) was slowly added, the reaction mixture was extracted with ethyl acetate and the organic layer was dried over anhydrous Mg_2SO_4. Solvents were evaporated and the residue was purified by column chromatography on silica gel to give the desired product **mdp** as a yellow solid (6.22 g, 81% yield).

Synthesis of $[(mdp)_2Ir(\mu\text{-}Cl)]_2$ (Scheme S1)

According to a modified Nonoyama procedure,[2] $IrCl_3 \cdot 3H_2O$ (3.53 g, 10.0 mmol), 4-methyl-2,5-diphenylpyridine (**mdp**) (7.35 g, 30.0 mmol), and a mixed solvent 2-methoxyethanol/water (3:1, v/v, 60 mL) were heated to reflux (~120 °C) for 30 h under nitrogen. After the reaction solution was cooled to room temperature, deionized water (200 mL) was slowly added and the resulting mixture was filtered. The precipitate was washed with deionized water

several times to provide the desired intermediate complex as a yellow solid (6.61 g, 92% yield) which was used without further purification.

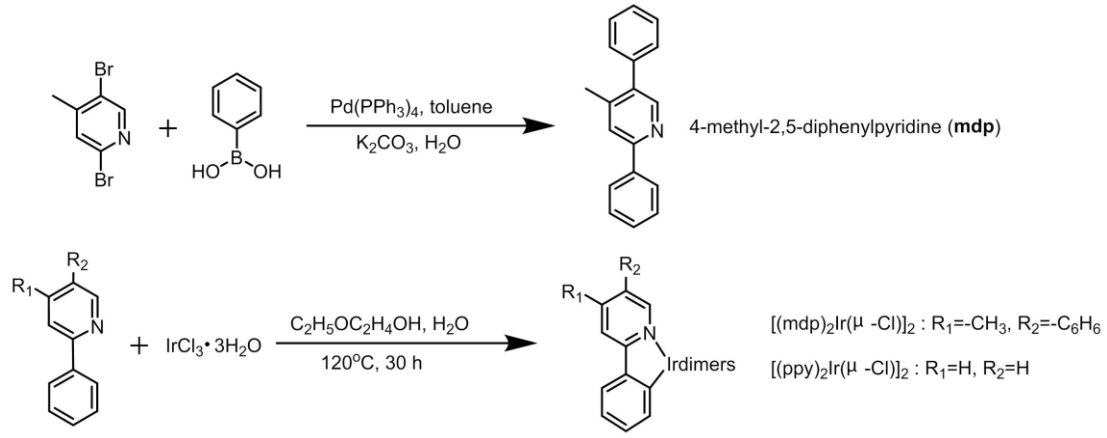

Scheme S1. The synthetic routes to the mdp ligand and two Ir-dimers.

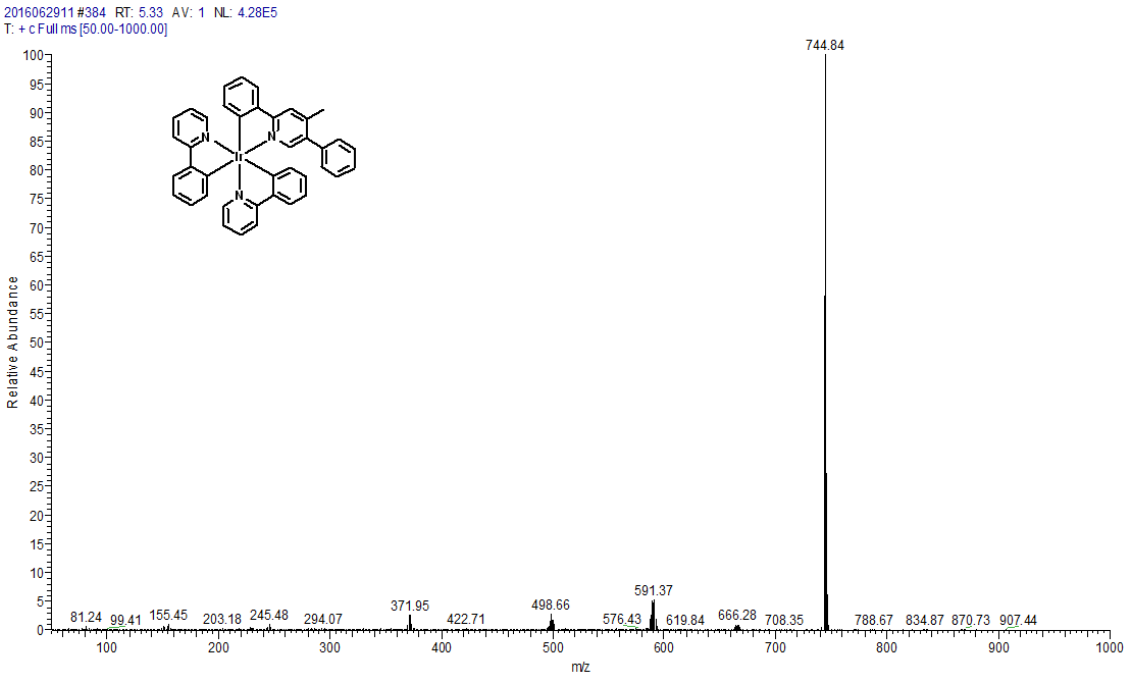

Figure S1. Mass spectrum of complex **3**.

10.1002/ejic.201800550

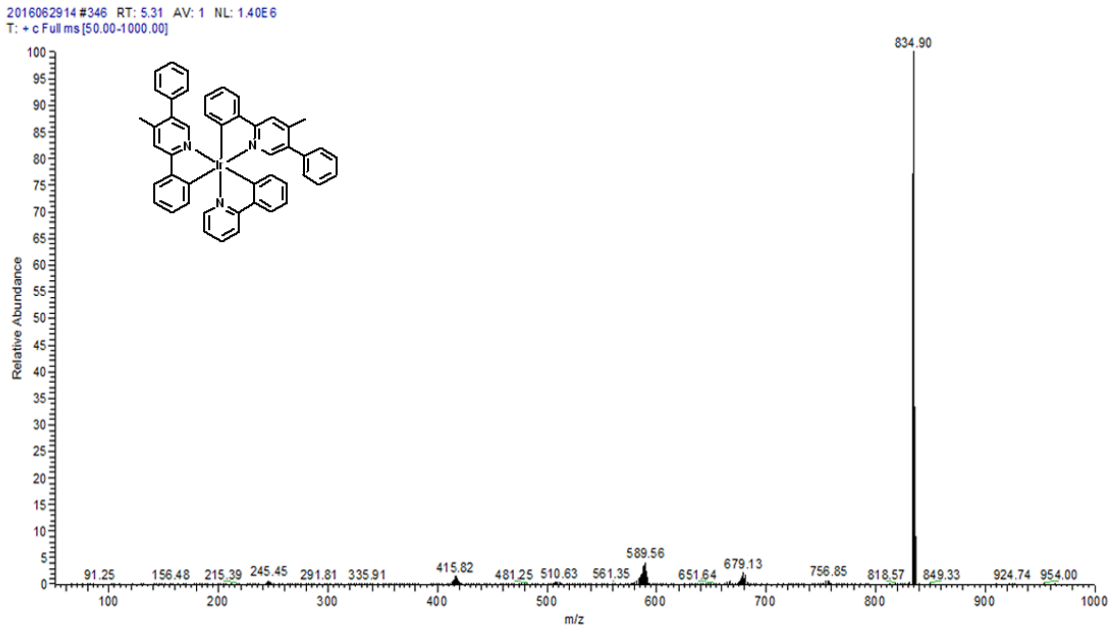

Figure S2. Mass spectrum of complex **4**.

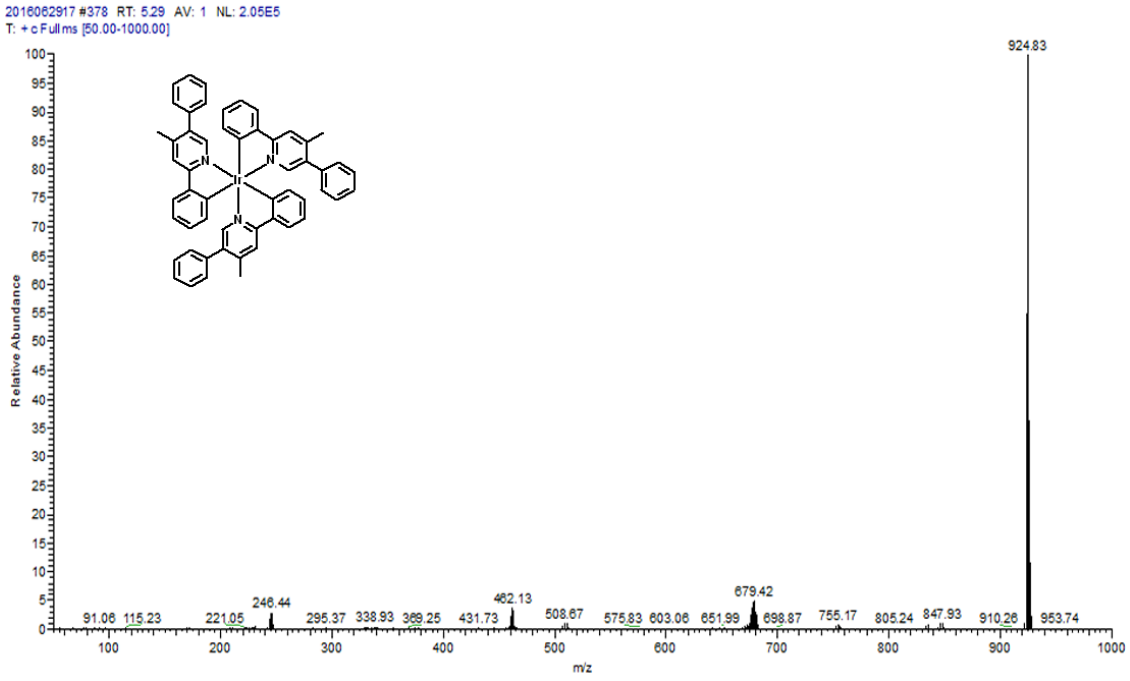

Figure S3. Mass spectrum of complex **5**.

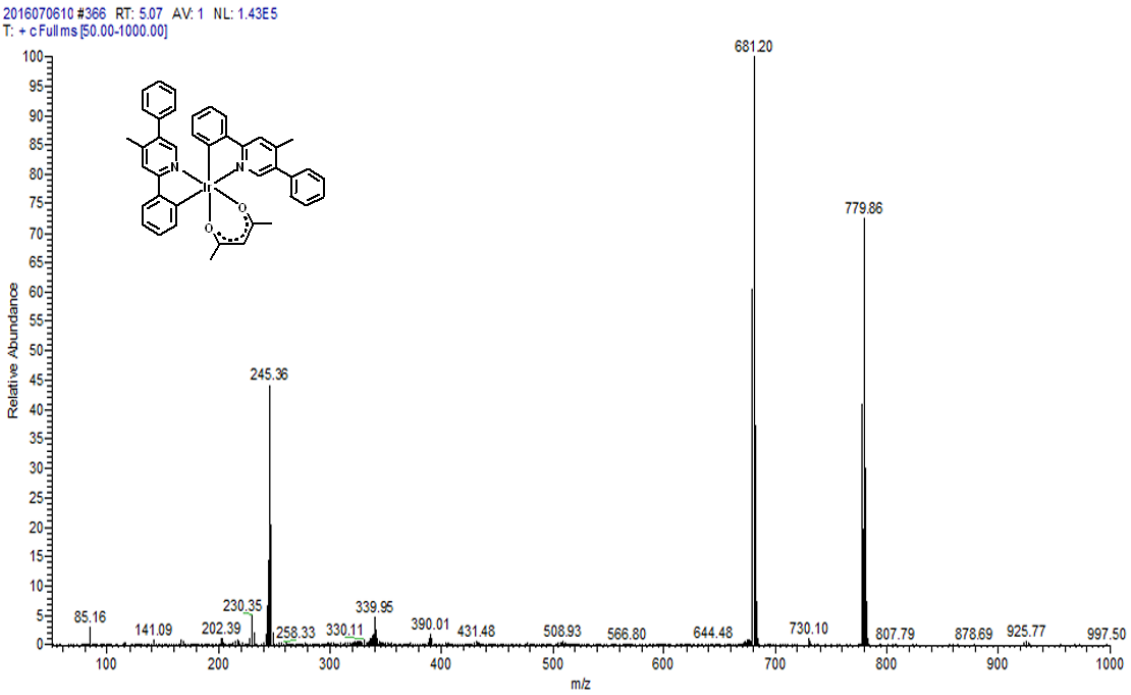

Figure S4. Mass spectrum of complex **6**.

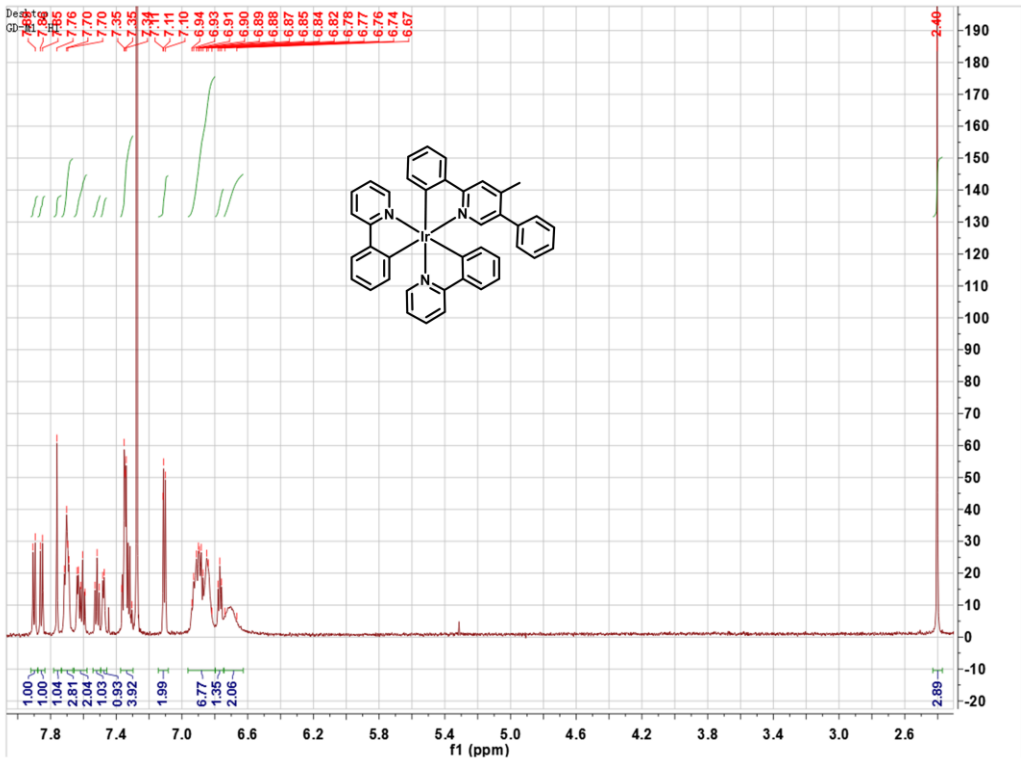

Figure S5. ^{1}H NMR spectrum of complex **3** in $CDCl_3$.

10.1002/ejic.201800550

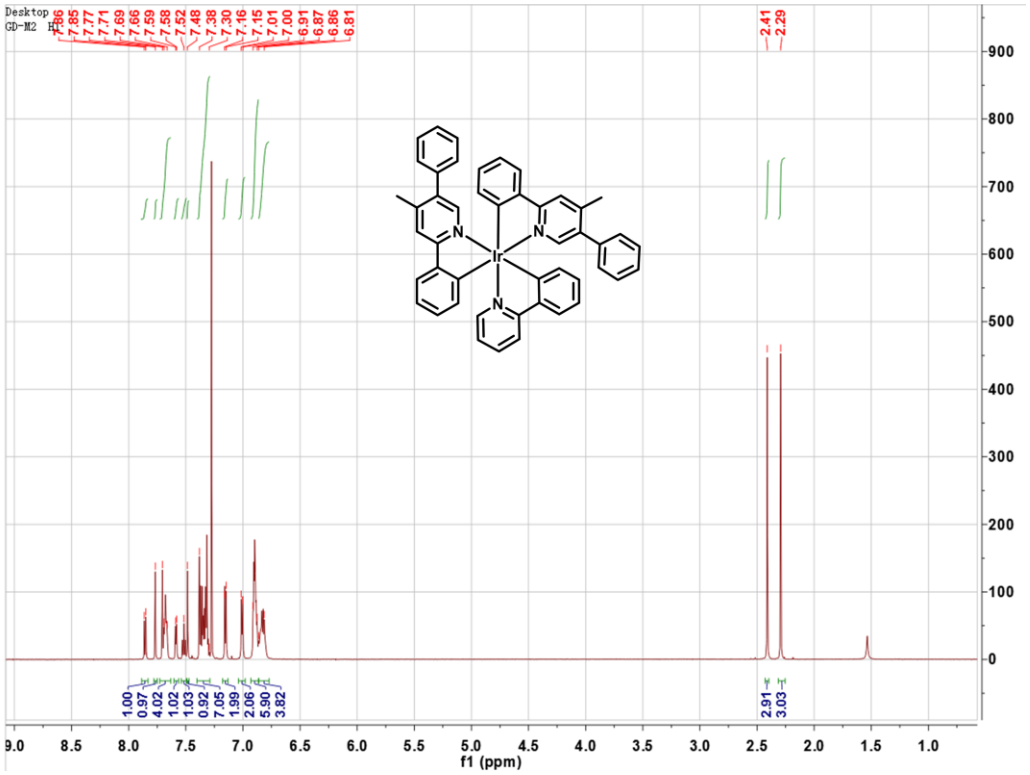

Figure S6. ^{1}H NMR spectrum of complex **4** in $CDCl_3$.

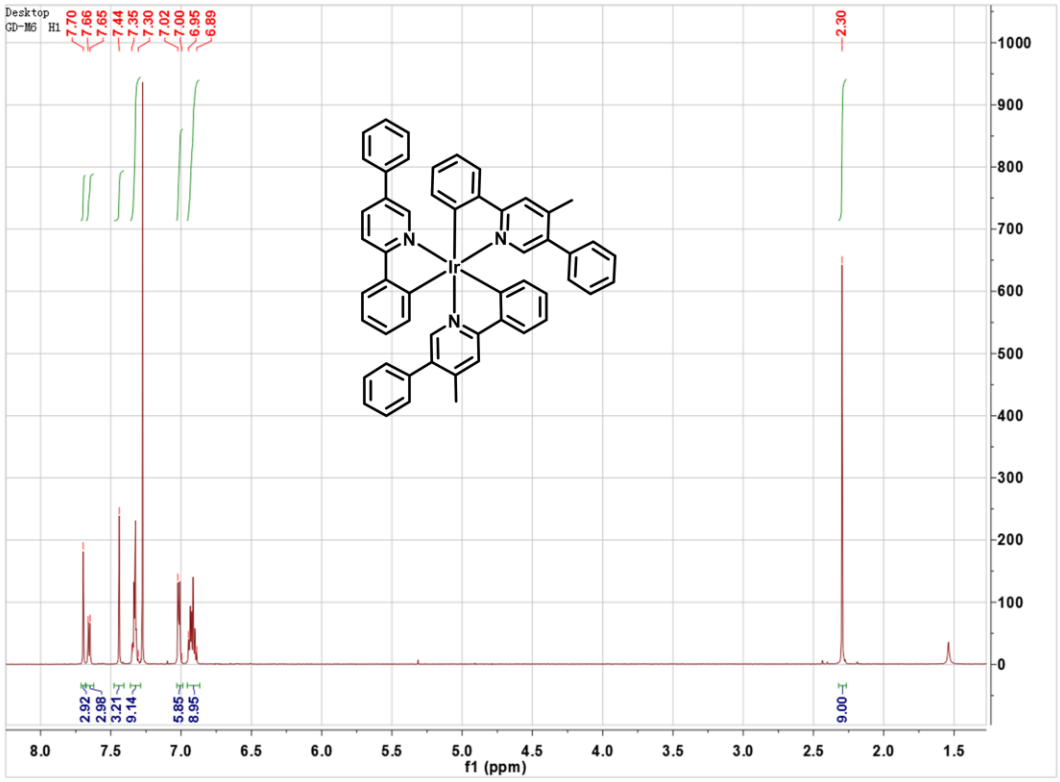

Figure S7. ^{1}H NMR spectrum of complex **5** in $CDCl_3$.

10.1002/ejic.201800550

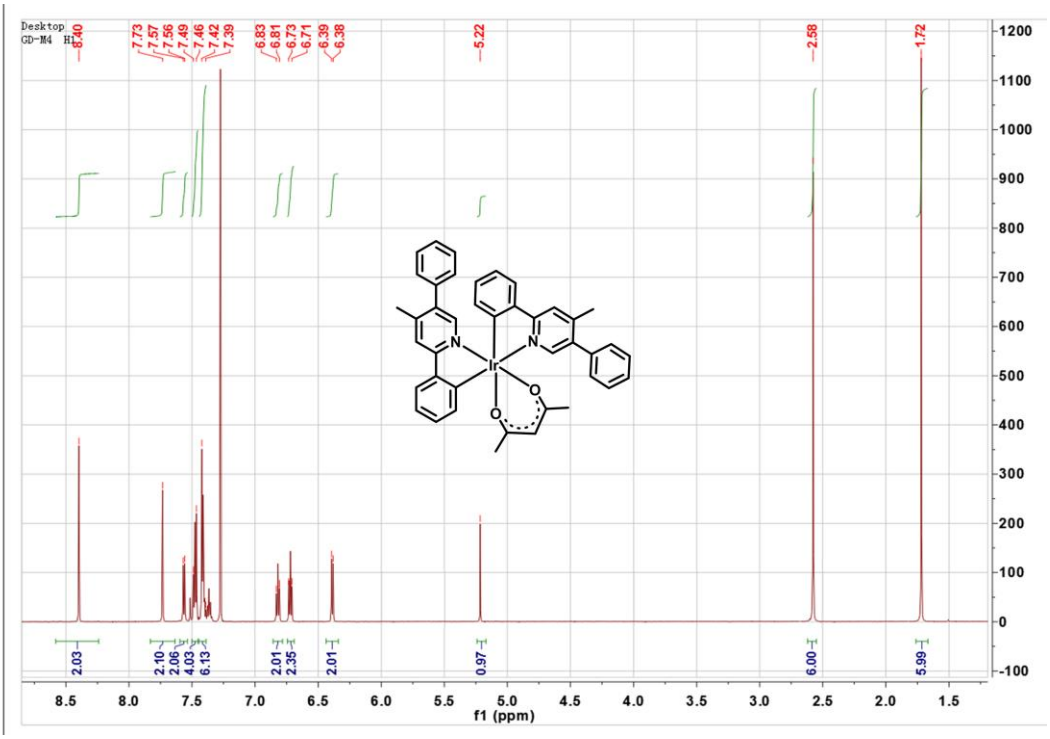

Figure S8. ^{1}H NMR spectrum of complex **6** in $CDCl_3$.

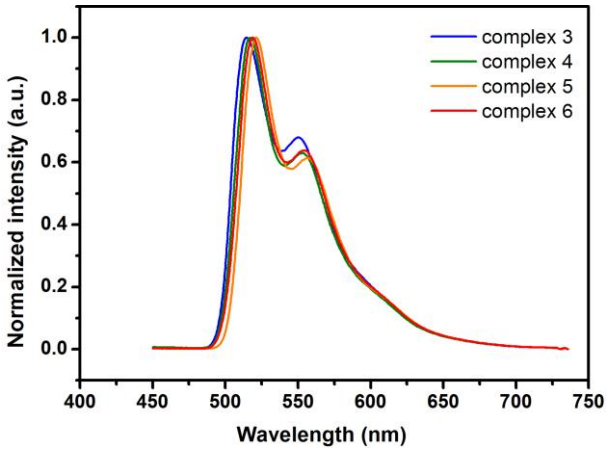

Figure S9. PL emission spectra of complexes **3-6** in toluene solution at 77 K.

Table S1. Crystal data

Compound	**3**	**4**	**6**
CCDC	1575648	1575649	1575651
Formula	$C_{40}H_{30}IrN_3$	$C_{47}H_{36}IrN_3$	$C_{41}H_{31}IrN_2O_2$
Formula Weight	744.87	865.99	860.80
Crystal System	monoclinic	monoclinic	monoclinic
a/Å	19.789(4)	8.8982(5)	9.8668(11)
b/Å	8.6212(16)	24.0087(12)	14.4002(16)
c/Å	18.170(3)	17.6619(9)	26.200(3)
α/°	90	90	90
β/°	106.696(3)	95.6220(10)	95.780(2)
γ/°	90	90	90
Z	4	4	4
R_1 [I>2σ(I)]	0.07	0.06	0.04
	Bond lengths [Å] and angles [deg]		
Ir(1)-N(1)	1.980(17)	2.127(7)	2.029(5)
Ir(1)-N(2)	2.053(16)	2.102(7)	2.026(5)
Ir(1)-N(3)	2.129(12)	2.123(7)	
Ir(1)-C(1)	2.111(13)	2.016(9)	
Ir(1)-C(6)	2.001(4)		1.993(6)
Ir(1)-C(12)	2.109(13)	2.023(8)	
Ir(1)-C(23)	1.995(15)		
Ir(1)-C(24)			
Ir(1)-C(30)		2.008(9)	
Ir(1)-O(1)			2.155(4)
Ir(1)-O(2)			2.151(4)

Fabrication of the OLEDs and EL Measurements

The devices were fabricated on glass substrates, which were patterned with indium tin oxide (ITO) having a sheet resistance equal to 20 Ω/square. The ITO glass was routinely cleaned by ultrasonic treatment in detergent solutions, followed by rinsing with deionized water and acetone. The glass was dried in a vacuum oven between each cleaning step above. The ITO substrate was treated using a Plasma Cleaner (PDC-32G-2, 100 W) with oxygen ambient to reduce the possibility of electrical shorts on the ITO anode and to increase the value of its work function. All the organic materials were purified by sublimation before depositing onto the ITO substrate at a rate of 0.3 Å s^{-1} without breaking the vacuum (~5.0×10^{-4} Pa). A very thin layer of LiF (0.5 nm) deposited at a rate of 0.1 Å s^{-1} was evaporated to enhance electron injection from the aluminum cathode. The finished Al electrode (cathode) was deposited at a rate of 4 Å s^{-1} and the active area of the diode segments was 2 x 3 mm^2. The EL spectra, brightness, CIE coordinates and current density-luminance-voltage characteristics of the devices were measured using a Photo Research PR650 spectrophotometer combined with a computer-controlled, programmable direct-current (DC) source (Keithley 2400).

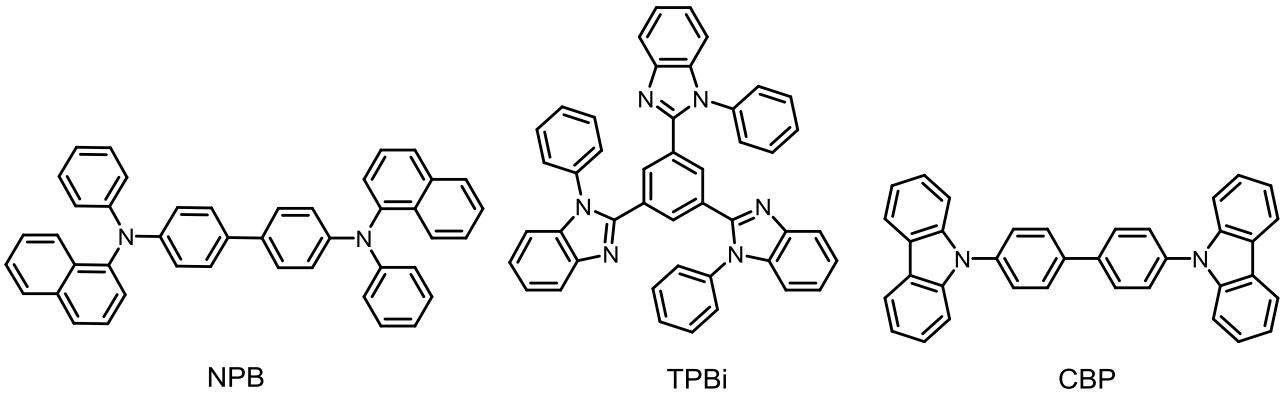

Figure S10. The chemical structures of the two transporting materials, NPB and TPBi, and the host material CBP.

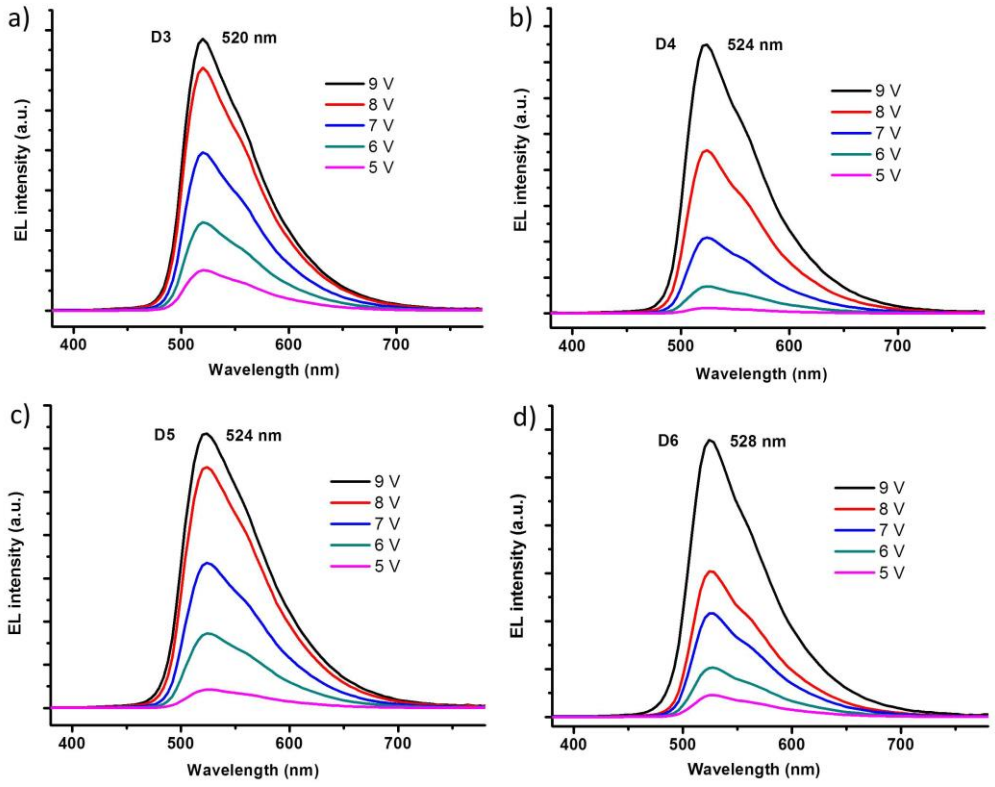

Figure S11. EL spectra a) **D3**, b) **D4**, c) **D5** and d) **D6** under the driving voltages of 5, 6, 7, 8 and 9 V, respectively.

References for SI.

[1] K. Hideo, T. Junichi, K. Rumi, M. Yasushi, *Jpn. Kokai Tokkyo Koho* (2017), JP 2017226633A.

[2] M. Nonoyama, *Bull. Chem. Soc. Jpn.* **1974**, *47*, 767-768.